

### Raman Spectra of Tetragonal $\text{KH}_2\text{PO}_4$ <sup>†</sup>

C. Y. She, T. W. Broberg, and David F. Edwards  
*Colorado State University, Fort Collins, Colorado 80521*  
 (Received 19 April 1971)

Raman spectra of crystalline  $\text{KH}_2\text{PO}_4$  at 294°K are reported for shifts up to 700  $\text{cm}^{-1}$ . Five of the six optical-phonon modes of the  $\text{K}^+(\text{H}_2\text{PO}_4)^-$  lattice are unequivocally identified; their positions and linewidths are accurately determined. Analysis of the spectral structures above 300  $\text{cm}^{-1}$  shows that the tetrahedral  $(\text{PO}_4)^{3-}$  ion remains essentially as an "individual" molecule in the crystal, and its vibrational modes are split by the local crystalline field of  $S_4$  symmetry.

Recent interest in the ferroelectric transition<sup>1</sup> and polarization fluctuations<sup>2</sup> of crystalline  $\text{KH}_2\text{PO}_4$  (KDP) suggests a need for investigating the optical-phonon spectra (lattice modes) of the crystal. Popova and Stekhanov<sup>3</sup> reported room-temperature laser-excited Raman spectra with the scattered polarization unanalyzed. They identified three of the six lattice modes of the  $\text{K}^+(\text{H}_2\text{PO}_4)^-$  lattice as predicted by simple group theory. We present in this paper Raman spectra of KDP at 294°K for shifts up to 700  $\text{cm}^{-1}$ ; the polarization of both incident and scattered radiation is analyzed to avoid possible ambiguity in spectral differentiation. Better resolution and much improved signal-to-noise ratio in our spectra allow us to (i) identify unequivocally five of the six optical-phonon modes, and (ii) report accurate linewidths as well as positions of these modes. In addition, we have also identified lines above 300  $\text{cm}^{-1}$  and their structure in all polarizations. Group-theoretical arguments lead us to conclude that the vibrational modes of the  $(\text{PO}_4)^{3-}$  ion in the KDP crystal are split under crystalline fields of the local symmetry  $S_4$ . These modes therefore remain essentially molecular vibrations.

The KDP crystal at room temperature may be regarded<sup>4</sup> as consisting of  $\text{K}^+$  and  $(\text{H}_2\text{PO}_4)^-$  ions belonging to the space group  $D_{2d}^{12}$ . The primitive cell for this model contains two  $\text{K}^+$  ions and two  $(\text{H}_2\text{PO}_4)^-$  ions, both occupying sites<sup>4,5</sup> of  $S_4$  symmetry. The point group of the crystal which depicts the long-wave optical phonons and the center of the Brillouin zone is  $D_{2d}$ . A simplified method<sup>6,7</sup> using the correlation table of point groups may be applied to determine the zone-center optical-phonon spectra. Each ion in the primitive cell may undergo translational motion with components along the  $z$  direction and in the  $xy$  plane. For the  $S_4$  sites which both the  $\text{K}^+$  and the  $(\text{H}_2\text{PO}_4)^-$  ions occupy, these motions belong to the  $B$  and  $E$  species, respectively. These species of the site group  $S_4$  are correlated with the irreducible representations of the crystal point group  $D_{2d}$  by the connecting arrows, according to

the correlation table.<sup>7</sup> A convenient format for carrying out this correlation is shown in Table I. In the center column all of the species of the crystal point group  $D_{2d}$  are listed. Only the translational species of the  $\text{K}^+$  and  $(\text{H}_2\text{PO}_4)^-$  ions which occupy the site group  $S_4$  are listed in the left and right columns of the table. The number of times a particular species occurs in the final decomposition is given by the number of arrows which terminate on that species symbol. In this manner, the lattice vibrations of KDP are decomposed into  $2B_1 + 2B_2 + 4E$  phonon modes of the lattice. The acoustical-phonon modes are the translational species  $B_2(T_x) + E(T_x, T_y)$  indicated in the table. Subtracting these from the total phonon modes, the remainder  $2B_1 + B_2 + 3E$  are the species corresponding to the optical-phonon modes. This classification agrees with the detailed analysis of Shur.<sup>8</sup>

Experimentally, a 50-mW He-Ne laser was used for excitation. The scattered light was analyzed with a Czerny-Turner double monochromator;

TABLE I. Correlation table of group  $D_{2d}$  and normal modes of the  $\text{K}^+(\text{H}_2\text{PO}_4)^-$  lattice.

$2\text{K}^+ - S_4$	$\text{KDP} - D_{2d}$	$2(\text{H}_2\text{PO}_4)^- - S_4$
	$A_1$	
	$A_2(R_z)$	
$B(T_z)$	$B_1$	$B(T_z)$
	$B_2(T_z)$	
$E(T_x, T_y)$	$E(T_x, T_y)$	$E(T_x, T_y)$
<b>Acoustical modes = <math>B_2 + E</math></b>		
<b>Optical modes = <math>2B_1 + B_2 + 3E</math></b>		

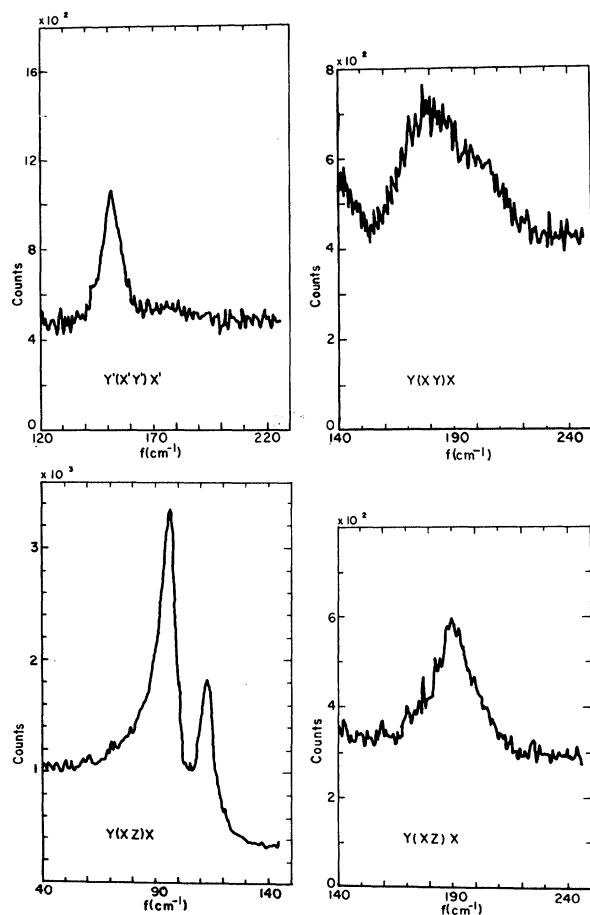


FIG. 1. Raman spectra of the  $\text{K}^+(\text{H}_2\text{PO}_4)^-$  lattice; linewidth of the instrumentation function is  $4 \text{ cm}^{-1}$ ;  $B_1$  mode at  $151 \text{ cm}^{-1}$ ,  $B_2$  mode at  $180 \text{ cm}^{-1}$ , and  $E$  modes at  $96$ ,  $114$ , and  $190 \text{ cm}^{-1}$ .

photon-counting detection techniques were used and the results were stored in a multichannel analyzer. A digital-timer circuit was constructed for the multichannel analyzer to increase the counting time. The intensity of our light source and the dispersion of our monochromator are comparable to those used by Popova and Stekhanov,<sup>3</sup> but the advantage of our detection system is that for a given spectral range we can dwell for a long time and thus increase the signal-to-noise ratio.<sup>9</sup> Two KDP samples of orthorhombic shape were used. The three mutually perpendicular edges of one crystal were parallel to the crystallographic axes  $x$ ,  $y$ , and  $z$ . The second crystal was fabricated such that the  $x'$  and  $y'$  edges were  $45^\circ$  with respect to the  $x$  and  $y$  axes, and the  $z$  edge remained as in the first crystal. This second orientation was chosen to help unscramble the resulting spectra. The scattering volume for the experiment was about  $1 \text{ cm} \times 2000 \mu^2$ .

The spectra in the region of the optical phonons of the  $\text{K}^+(\text{H}_2\text{PO}_4)^-$  lattice are shown in Fig. 1.

The slit width used was  $200 \mu$  which gives a measured linewidth of  $4 \text{ cm}^{-1}$  for the instrument function. The notation for the incident and scattered polarizations is conventional<sup>10</sup>:  $y(xz)x$ , for example, indicates a measurement of the intensity of the Raman tensor element  $\alpha_{xx}$  scattering along the  $x$  axis with light incident in the  $y$  direction. The intensity scale in the figure refers to experimental photon counts. According to the symmetry of the Raman tensors<sup>7</sup> for the point group  $D_{2d}$  given in Table II, five of the six lattice modes of the various symmetry species are identified. The position and the full linewidth at half-maximum,  $\Delta f$ , of the Raman-active lines in Fig. 1 are readily determined. They are  $151$  ( $\Delta f = 10$ ) for the  $B_1$  mode,  $180$  ( $\Delta f = 27$ ) for the  $B_2$  mode, and  $96$  ( $\Delta f = 9$ ),  $114$  ( $\Delta f = 7$ ),  $190$  ( $\Delta f = 21$ ) for the  $E$  modes, all in  $\text{cm}^{-1}$ . The quality of our spectra in Fig. 1 is obviously superior to that reported by Popova and Stekhanov,<sup>3</sup> whose quoted width for the instrument function is  $6 \text{ cm}^{-1}$  in this spectral region. Owing perhaps to the lack of scattered signal, Popova and Stekhanov did not analyze the polarization of the scattered radiation, and as a result they were unable to resolve the broad  $B_2$  mode at  $180 \text{ cm}^{-1}$  from the  $E$  mode at  $190 \text{ cm}^{-1}$ . Their early data<sup>11</sup> showed a line at  $58 \text{ cm}^{-1}$  and it was included as an  $E$  mode in Shur's calculation.<sup>8</sup> Since they could not locate this line in their recent work,<sup>3</sup> and neither can we find this line, its existence is questionable. The three  $E$  modes we report here are probably the only optical lattice modes of  $E$  species as predicted by group theory. The only optical lattice mode yet unfound is a  $B_1$  mode which is either very weak or has a frequency of less than  $4 \text{ cm}^{-1}$ . We have searched for this mode down to a shift of  $4 \text{ cm}^{-1}$  without success.

The spectra in Fig. 2 were taken with a measured  $7\text{-cm}^{-1}$  linewidth for the instrument function and cover frequency shifts up to  $700 \text{ cm}^{-1}$ . The  $y(xy)x$  spectrum in Fig. 2(c) is in agreement with the spectrum given by Kaminow<sup>2</sup> in which he made no attempt to identify the optical modes of the  $\text{K}^+(\text{H}_2\text{PO}_4)^-$  lattice. In general, our spectra in Fig. 2 show several detailed features. There is a shoulder in the  $y(xy)x$  spectrum and a high background in the  $y(xz)x$  spectrum in the low-frequency region. The causes for these features and for other askew lines could perhaps be explained in terms of anharmonic interactions. In particular, the broad left shoulder of the  $470\text{-cm}^{-1}$  line may be due to the existence of weaker lines in that region,<sup>3</sup> but we were unable to resolve the details. The lines below  $300 \text{ cm}^{-1}$  are the optical lattice modes detailed in Fig. 1. The strong peaks above  $300 \text{ cm}^{-1}$  may be associated with the internal vibrations<sup>12</sup> of the  $(\text{H}_2\text{PO}_4)^-$  ion.

It is well known<sup>13</sup> that the vibrational modes of a

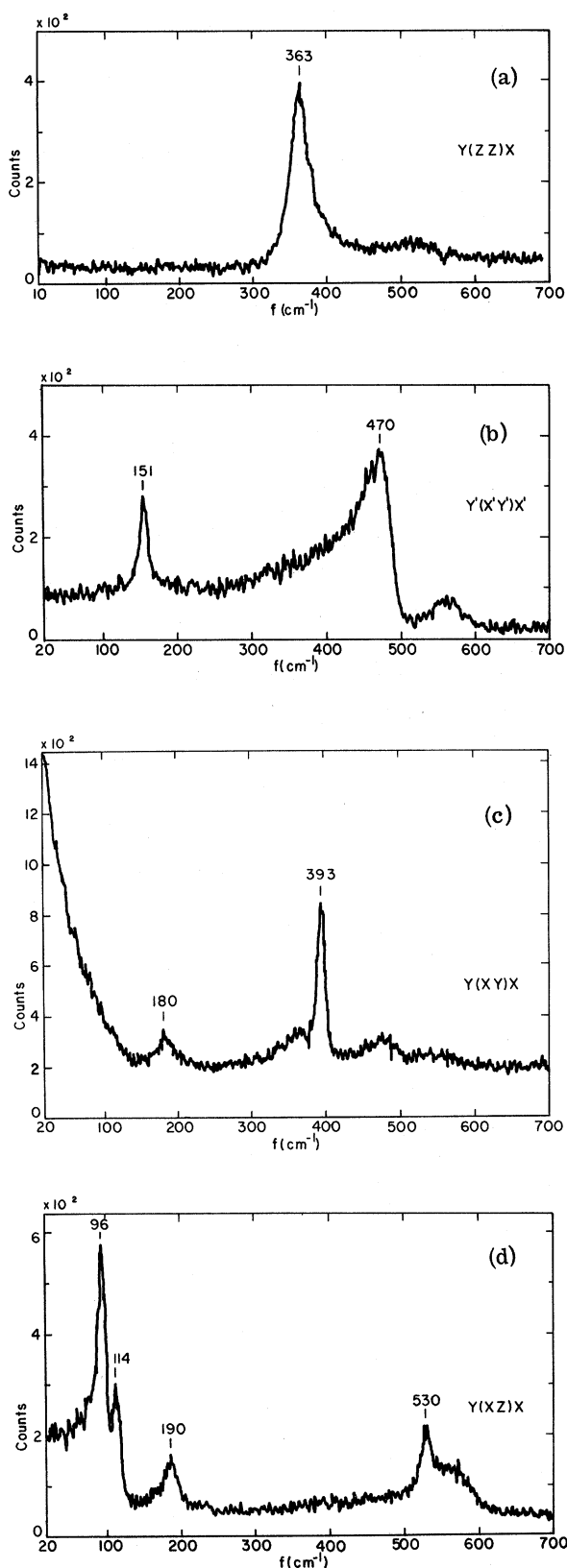


FIG. 2. Raman spectra of KDP; (a)  $A_1$  species, (b)  $B_1$  species, (c)  $B_2$  species, and (d)  $E$  species.

free tetrahedral  $(\text{PO}_4)^{3-}$  ion consist of an  $A_1$  mode at  $980 \text{ cm}^{-1}$ , an  $E$  mode at  $363 \text{ cm}^{-1}$ , and two  $F_2$  modes at  $515$  and  $1082 \text{ cm}^{-1}$ . All of these species of the point group  $T_d$  are Raman active. Whether the phosphate ion behaves essentially as an "individual" molecule in the crystalline KDP deserves some investigation. If the phosphate ion binds strongly with the lattice as does the  $\text{SiO}_2$  molecule in a quartz crystal,<sup>14</sup> one would expect the original molecular vibrations to disappear and new lattice modes with species under the crystal point group symmetry  $D_{2d}$  to be formed. Our polarized Raman data in Fig. 2 do not suggest this to be the case. The lines shown in Fig. 2 near  $363$  and  $515 \text{ cm}^{-1}$  are characteristic of the molecular vibrations of the  $(\text{PO}_4)^{3-}$  ion modified slightly by the surrounding crystalline field. Owing to this small perturbation, the  $E$  mode of  $T_d$  symmetry of the  $(\text{PO}_4)^{3-}$  ion at  $363 \text{ cm}^{-1}$  is split into lines at  $363$  and  $393 \text{ cm}^{-1}$  in the crystal. Similarly, the  $F_2$  mode of the tetrahedral  $(\text{PO}_4)^{3-}$  ion at  $515 \text{ cm}^{-1}$  is split into lines at  $470$  and  $530 \text{ cm}^{-1}$ . In Table II we decompose the  $E$  and  $F_2$  modes of  $T_d$  symmetry into species of the point groups of lower symmetry  $D_{2d}$  and  $S_4$ . Such decomposition and the transformation of Raman tensors given in the table are well known from group theory.<sup>7</sup> By comparing the Raman spectra with the tensors listed, we can determine which is the correct decomposition and thus detect what has happened to the  $(\text{PO}_4)^{3-}$  ion in the crystal. For example, the  $393\text{-cm}^{-1}$  line ( $E$  mode) appears in the  $y(xy)x$  spectrum but not in the  $y'(x'y')x'$  spectrum of Fig. 2 corresponding to Raman tensor element  $\alpha_{xy}$  but not element  $\alpha_{x'y'}$ . From Table II we can see that the  $393\text{-cm}^{-1}$  line corresponds to the  $B$  species of the  $S_4$  group, and not  $B_1$  species of the  $D_{2d}$  group. Similarly, the  $470\text{-cm}^{-1}$  line ( $F_2$  mode) appears in the  $y'(x'y')x'$  spectrum and not the  $y(xy)x$  spectrum of Fig. 2, indicating that this line corresponds to the  $B$  species of group  $S_4$  and not the  $B_2$  species of the  $D_{2d}$  group. Therefore, the local crystalline field in KDP causes the  $E$  and  $F_2$  vibrations of the  $(\text{PO}_4)^{3-}$  ion to split into  $A+B$  and

TABLE II. Spectral decomposition for the  $(\text{PO}_4)^{3-}$  ion under crystalline field and the Raman tensors of the point groups  $D_{2d}$  and  $S_4$ .

	$D_{2d}$	$T_d$	$S_4$
$(\alpha_{xx} + \alpha_{yy}, \alpha_{zz})$	$A_1$	E	A $(\alpha_{xx} + \alpha_{yy}, \alpha_{zz})$
	$A_2$		
$(\alpha_{xx} - \alpha_{yy}, \alpha_{xy})$	$B_1$	E	B $(\alpha_{xx} - \alpha_{yy}, \alpha_{xy})$
	$B_2$		
$(\alpha_{xy})$		$F_2$	
$(\alpha_{yz}, \alpha_{zx})$	E		E $(\alpha_{yz}, \alpha_{zx})$

$B+E$  vibrational modes of the  $S_4$  symmetry, respectively. The motion of the constituent atoms must, of course, comply with the space group symmetry of the crystal and the two  $B$  species of  $S_4$  symmetry, according to Table I, are correlated into the  $B_1+B_2$  zone-center phonons. All these

modes behave essentially as "individual" molecular vibrations and may be considered as examples of Einstein phonons.

The authors wish to acknowledge the assistance of Vaughn Draggoo for his help in the initial stages of these experiments.

†This work was sponsored in part by a contract with the Air Force Cambridge Research Laboratories, Office of Aerospace Research, USAF.

<sup>1</sup>E. M. Brody and H. Z. Cummins, in *Light Scattering Spectra of Solids*, edited by G. B. Wright (Springer, New York, 1969), p. 683; E. Litov and E. A. Uehling, *Phys. Rev. B* **1**, 3713 (1970).

<sup>2</sup>I. P. Kaminow, in *Light Scattering Spectra of Solids*, edited by G. B. Wright (Springer, New York, 1969), p. 675.

<sup>3</sup>E. A. Popova and A. I. Stekhanov, *Fiz. Tverd. Tela* **12**, 51 (1970) [*Sov. Phys. Solid State* **12**, 40 (1970)].

<sup>4</sup>F. Jona and G. Shirane, *Ferroelectric Crystals* (Pergamon, New York, 1962); R. Wyckoff, *Crystal Structures*, 2nd ed. (Interscience, New York, 1963), Vol. III.

<sup>5</sup>*International Tables for x-Ray Crystallography*, 3rd ed., edited by N. F. M. Henry and K. Lonsdale (Kynoch Press, New York, 1969), Vol. I.

<sup>6</sup>R. K. Khanna and C. W. Reimann, *Spectra-Physics Raman Tech. Bull. No. 3*, 1970 (unpublished); W. G. Fateley, N. T. McDevitt, and F. F. Bentley, *Appl. Spectry*, **25**, 155 (1971).

<sup>7</sup>J. P. Mathieu, *Spectre de Vibration et Symmetrie des Molécules et des Cristaux* (Hermann, Paris, France, 1945); E. Wilson, J. Decius, and P. Cross, *Molecular Vibrations* (McGraw-Hill, New York, 1955).

<sup>8</sup>M. Shur, *Fiz. Tverd. Tela* **8**, 57 (1966) [*Sov. Phys. Solid State* **8**, 43 (1966)].

<sup>9</sup>Y. D. Harker, Jon D. Masso, and D. F. Edwards, *J. Appl. Optics* **8**, 2563 (1969).

<sup>10</sup>T. C. Damen, S. P. S. Porto, and B. Tell, *Phys. Rev.* **142**, 570 (1966).

<sup>11</sup>A. I. Stekhanov and E. A. Popova, *Fiz. Tverd. Tela* **7**, 3530 (1965) [*Sov. Phys. Solid State* **7**, 2849 (1966)].

<sup>12</sup>J. P. Chapelle, *J. Chem. Phys.* **46**, 30 (1949); I. P. Kaminow, R. C. C. Leite, and S. P. S. Porto, *J. Phys. Chem. Solids* **26**, 2085 (1965).

<sup>13</sup>See, for example, G. Herzberg, *Infrared and Raman Spectra of Polyatomic Molecules* (Van Nostrand, Princeton, N. J., 1945).

<sup>14</sup>J. D. Masso, C. Y. She, and D. F. Edwards, *Phys. Rev. B* **1**, 4179 (1970); C. Y. She, J. D. Masso, and D. F. Edwards, *J. Phys. Chem. Solids* (to be published).

## Average Magnetic Hyperfine Fields at $^{106}\text{Pd}$ Nuclei in Ni-Pd Alloys

M. M. El-Shishini, \* R. W. Lide, Paul G. Huray, and J. O. Thomson

*Department of Physics and Astronomy, University of Tennessee, Knoxville, Tennessee 37916*

(Received 9 April 1971)

The average magnetic hyperfine fields at  $^{106}\text{Pd}$  nuclei in a series of Ni-Pd alloys have been measured at 77°K by means of the integral perturbed-angular-correlation method using the (622.0–511.8)-keV  $\gamma$ -ray cascade in  $^{106}\text{Pd}$ . The observed magnetic fields have been corrected for the external applied field and the sample magnetization, and extrapolated to 0°K. The average hyperfine fields  $H_{\text{hf}}$  at the Pd nuclei were found to be negative in the ferromagnetic alloys over the full concentration range, varying from  $(-194 \pm 9)$  kG in Ni metal to  $(-41 \pm 10)$  kG in an alloy of 90% Pd. Our estimates for the contribution to the hyperfine field of Pd arising from the local moment on the Pd atom are too small to account for the net measured fields. Thus, we ascribe the origin of the remaining large negative fields to interactions with neighboring atoms through the conduction electrons.

### I. INTRODUCTION

The magnetic properties of palladium metal and its alloys have been the subject of considerable study, particularly in the last few years. Among the most interesting properties is the occurrence of ferromagnetism in Pd alloyed with very small concentrations of Fe, Co, and Ni.<sup>1,2</sup> At these small concentrations of the  $3d$  metal, susceptibility and neutron studies have indicated that giant moments

are associated with each impurity atom.<sup>1-3</sup> These moments, up to  $12 \mu_B$  per impurity atom, are much greater than can be produced by  $3d$  states on the impurity alone. Thus, it is reasonable to assume that the Pd atoms nearby one of these impurities carry a moment and are intimately associated with the long-range ferromagnetic coupling observed for alloys with these small concentrations of  $3d$  metal. The part played by conduction electrons in the long-range ferromagnetic coupling between impurities is,